Gene Expression Patterns 11 (2011) 12–21

Contents lists available at ScienceDirect

Gene Expression Patterns

journal homepage: www.elsevier.com/locate/gep

Identification of adult midgut precursors in Drosophila

Craig A. Micchelli [a,*,1], Lisa Sudmeier [a,1], Norbert Perrimon [b], Shan Tang [b], Ryan Beehler-Evans [a]

[a] Washington University School of Medicine, Department of Developmental Biology, Campus Box 8103, 660 South Euclid Avenue, St. Louis, MO 63110, United States
[b] Harvard Medical School, Howard Hughes Medical Institute, Department of Genetics, 77 Avenue Louis Pasteur, Boston, MA 02175, United States

ARTICLE INFO

Article history:
Received 22 June 2010
Received in revised form 18 August 2010
Accepted 19 August 2010
Available online 23 September 2010

Keywords:
Drosophila
Adult midgut precursors
Intestinal stem cell
Ecdysone

ABSTRACT

The adult *Drosophila* midgut is thought to arise from an endodermal rudiment specified during embryogenesis. Previous studies have reported the presence of individual cells termed adult midgut precursors (AMPs) as well as "midgut islands" or "islets" in embryonic and larval midgut tissue. Yet the precise relationship between progenitor cell populations and the cells of the adult midgut has not been characterized. Using a combination of molecular markers and directed cell lineage tracing, we provide evidence that the adult midgut arises from a molecularly distinct population of single cells present by the embryonic/larval transition. AMPs reside in a distinct basal position in the larval midgut where they remain through all subsequent larval and pupal stages and into adulthood. At least five phases of AMP activity are associated with the stepwise process of midgut formation. Our data shows that during larval stages AMPs give rise to the presumptive adult epithelium; during pupal stages AMPs contribute to the final size, cell number and form. Finally, a genetic screen has led to the identification of the Ecdysone receptor as a regulator of AMP expansion.

Stem cells are among the most primitive cells of a lineage and distinguished by the properties of self-renewal and multipotency. These attributes make stem cells ideally suited to generate functional organ systems during development and, perhaps too, in ex vivo culture. Understanding where and when stem and progenitor cell populations expand as they traverse a changing cellular environment in developmental time is critical to identifying the factors that regulate proliferation.

The size, accessibility and persistence of the *Drosophila* midgut from embryo to adult are all attributes that permit a time resolved analysis of midgut progenitor cells. In addition, recent studies have shown that intestinal stem cells (ISCs) can be identified in the adult midgut that function to maintain tissue homeostasis (Micchelli and Perrimon, 2006; Ohlstein and Spradling, 2006). Thus, we sought to identify early adult midgut progenitors (AMPs), determine if their numbers and position change throughout the course of development, and identify signals that regulate these processes.

Early studies have suggested that precursors of the adult insect midgut (AMPs) can be identified in the embryo as single cells. Transplantation experiments using *Drosophila* embryos have demonstrated the presence of single "spindle cells" interspersed among cells of the embryonic midgut by stage 16 (Technau and Campos-Ortega, 1986; Hartenstein et al., 1992). A diminutive cell size has also been used as a marker for precursor cells (Tepass and Hartenstein, 1994, 1995). Finally, expression of *pros* at embryonic stage 11 (Oliver et al., 1993; Spana and Doe, 1995; Hirata et al., 1995) and Achaete Scute Complex (AS-C) genes at stage 11 and 12 (Brand et al., 1993; Tepass and Hartenstein, 1995) have also been suggested to mark a population of individual AMPs. Early observations in *muscadea* suggested that individual precursors could be identified at early larval stages, as well, interspersed among large epithelial cells (Kowalevsky, 1887; Perez, 1910). Finally, there are numerous references to clusters of cells distributed throughout the *Drosophila* midgut, alternately referred to as imaginal midgut islands or islets (e.g. Skaer, 1993).

Despite its conspicuous anatomical presence, interest in the post-embryonic midgut has been largely incidental. Up until now, there have been few studies focused on larval AMPs or midgut islands, per se (Jiang and Edgar, 2009; Mathur et al., 2010). Recent studies have shown that *escargot* (*esg*) is expressed in AMPs during larval stages and that proliferation of AMPs depends on the EGFR/RAS/MAPK signaling pathway (Jiang and Edgar, 2009). Yet, many questions remain including the precise lineage relationship between *esg* expressing cells in the larvae and the cells of the adult midgut, if there are quantitative changes in AMP number throughout larval and pupal stages, the relationship between AMP position and the overall events of midgut morphogenesis, and whether additional signaling pathways regulate AMP expansion. In this study, we investigate these issues. First, we demonstrate that at least three distinct classes of small midgut cells can be defined in the midgut at the embryonic/larval transition on the basis of differential marker gene expression; esg^{+}Pros^{-}, esg^{+},

* Corresponding author. Tel.: +1 314 362 7036; fax: +1 314 362 7058.
E-mail address: micchelli@wustl.edu (C.A. Micchelli).
[1] Both authors contributed equally to this paper.

1567-133X/$ - see front matter © 2010 Elsevier B.V. All rights reserved.
doi:10.1016/j.gep.2010.08.005

Pros$^+$ and *esg*$^-$Pros$^+$. Second we show that each of these three classes of cells display distinct profiles of expansion and/or loss from the epithelium during larval and pupal stages. Importantly, one of the cell types, *esg*$^+$Pros$^-$, undergoes a series of four separable phases of cellular expansion. Third, using directed lineage-tracing analysis we define *esg*$^+$Pros$^-$ cells at the embryonic/larval transition as AMPs based on the capacity to produce the adult midgut. Finally, a genetic screen has led to the identification of the Ecdysone receptor (EcR) as a regulator of AMP expansion.

1. Results

1.1. Molecularly distinct cell types of the early larval midgut

We reasoned that if ISCs or their precursors are present in the post-embryonic midgut, then they might be identified based on common molecular and morphological criteria. Several candidate genes were assayed. Previous studies have shown that the transcription factor encoded by *escargot* (*esg*) is expressed in the adult ISCs, a population of cells with small nuclei located in a basal position in the tissue adjacent to the basement membrane and visceral musculature (Micchelli and Perrimon, 2006). In addition, studies of the *Drosophila* embryo have suggested that AMPs can be detected by *prospero* (*pros*) in the embryonic midgut at stage 11 (Oliver et al., 1993; Spana and Doe, 1995; Hirata et al., 1995) and *asense* (*ase*) at embryonic stage 12 (Brand et al., 1993). To determine if these markers define distinct populations of cells in the early midgut, we performed double labeling experiments. Our studies indicate that three distinct populations of small cells can be detected in the midgut at the embryonic/larval transition (see methods for staging); *esg*$^+$Pros$^-$, *esg*$^-$Pros$^+$, *esg*$^+$Pros$^+$ (double positive) cells (Fig. 1A–C). Quantification revealed that the average number of cells at 24 h AED is 45, 159, and 98 respectively (Fig. 1C). Finally, while Ase$^+$ cells were detected in the first instar nervous system, specific anti-Ase staining was not detected in the midgut (data not shown). Thus, three distinct populations of small cells can be detected in the early larval midgut.

To determine the contribution of these distinct cell populations to the adult midgut, we first performed a time resolved quantification of each cell type from the embryonic/larval transition to the end of pupal development, spanning nine successive 24 h intervals (Fig. 1C). These data show that two of the defined cell populations, *esg*$^-$Pros$^+$, *esg*$^+$Pros$^+$, are present in relatively low abundance throughout the course of the larval stages (Fig. 1C). Interestingly, at 24 h APF neither *esg*$^-$Pros$^+$ or *esg*$^+$Pros$^+$ cells were detected; by 72 h APF (P5) both cell populations were again present (Fig. 1C).

In contrast, the number of *esg*$^+$Pros$^-$ cells was highly dynamic. Five distinct activity phases could be discerned during larval and pupal development (P1–5; Fig. 1C). In P1 the average number of *esg*$^+$Pros$^-$ cells increased from 45 to 1096. During P1, *esg*$^+$Pros$^-$ cells were dispersed along the length of the midgut as single basally located cells (Fig. 1B; Supplemental Fig. 1). In early P2, single *esg*$^+$Pros$^-$ cells can be detected. However throughout P2 *esg*$^+$Pros$^-$ cells begin to form closely associated cell clusters (Fig. 1C, asterisks; Fig. 3B; Fig. 4A–G).

Quantification of cells per cluster at early P3 reveals that each cluster contains between 2 and 16 cells with detectable regional differences (Supplemental Fig. 2). P3 showed a precipitous loss of *esg*$^+$Pros$^-$ cells from 1150 clusters to 434 single *esg*$^+$Pros$^-$ cells (Fig. 1C). However, beginning at P4 the *esg*$^+$Pros$^-$ cell population began to expand, roughly doubling in number (Fig. 1C). While *esg*$^+$Pros$^-$ cell numbers continue to slowly increase during P5 attaining an average number of 1037, this increase is now accompanied by the reappearance of both *esg*$^-$Pros$^+$, *esg*$^+$Pros$^+$ cells (Fig. 1C; Supplemental Fig. 4). Thus, *esg*$^+$Pros$^-$ cells undergo four phases of expansion and a single contraction during post-embryonic development.

1.2. Lineage tracing defines AMPs

To determine which, if any, of the defined midgut cell populations correspond to AMPs we conducted a series of genetic lineage tracing experiments. We first asked whether there is a direct lineage relationship between any of the cells detected at P1 and the clusters present at P2. The MARCM system (Lee and Luo, 1999)

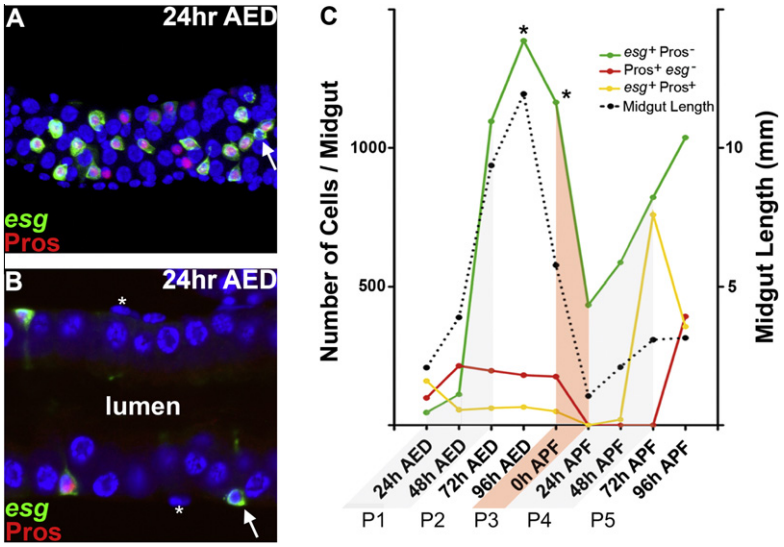

Fig. 1. Molecular markers define larval and pupal midgut cell types. (A) Three distinct populations of small cells can be defined in early first instar (24 h AED) *esg > GFP* midguts (anti-GFP, green; anti-Pros, red; DAPI, blue); *esg*$^+$Pros$^-$, Pros$^+$*esg*$^-$, *esg*$^+$Pros$^+$. Arrow indicates *esg*$^+$Pros$^-$ cell. Original magnification, 160×. (B) Small cells occupy a basal position in the early first instar midgut (arrow). Surrounding visceral muscle nuclei indicated with asterisk. Original magnification, 252×. (C) The dynamics of small cell subtypes from embryogenesis to adulthood in the midgut. Five phases (P1–5; shading) can be distinguished. Asterisk's indicate the number of clusters, not single cells. AED; after egg deposition; APF; after puparium formation.

was used to positively label P1 cells with GFP through induced mitotic recombination. Experiments in which midgut cells were labeled at P1 with a short heat pulse and examined in late P2 showed that labeled clusters could be detected (Fig. 2A). In

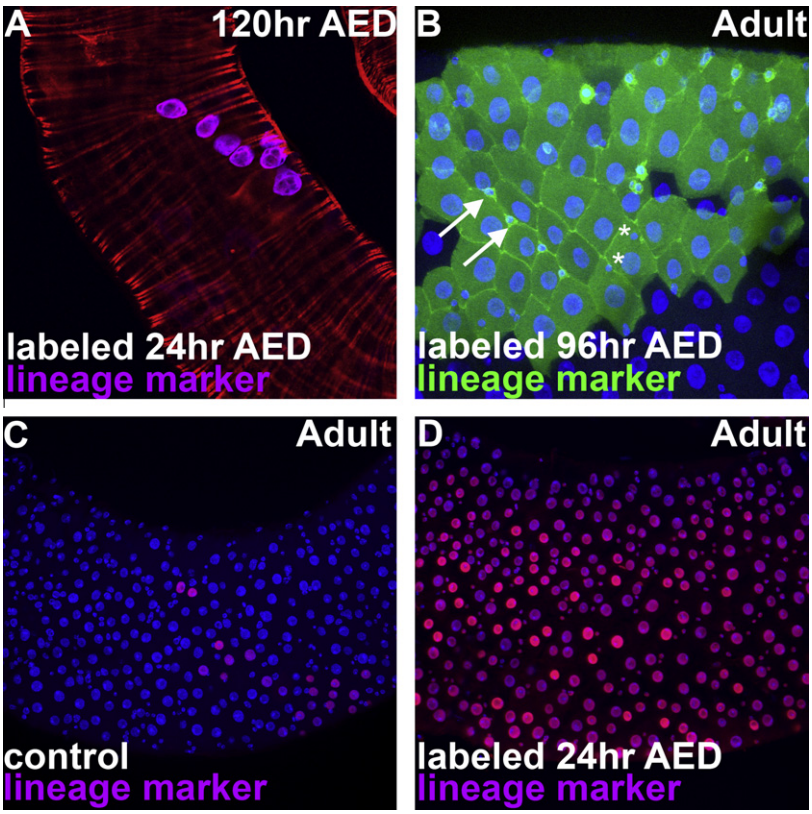

Fig. 2. Cell lineage tracing defines AMPs. (A and B) The MARCM system was used to positively identify ISC lineages with GFP (anti-GFP, green). (A) 120 h AED midgut labeled in P1 (24 h AED); phalloidin counterstain (red). Seven individual cell clusters are labeled. Original magnification, 40×. (B) An adult midgut labeled in mid P2 (96 h AED). Marked cells can be detected in broad regions of the adult midgut that label distinct cells types. Arrows indicate progenitor cells and asterisks indicate differentiated cells of the adult midgut. Original magnification, 80×. (C and D) Directed lineage tracing of midgut cells using the *act > stop > LacZ*^{nuc} label (anti-βgal, red; DAPI, blue). Original magnification, 40×. (C and D) Adult *esg*^{TS}/*act > stop > LacZ*^{nuc}; UAS-flp midguts. (C) Unshifted control. Some samples display low background labeling. (D) Adult midgut, which received a P1 (24 h AED) labeling pulse. Note extensive labeling of adult midgut.

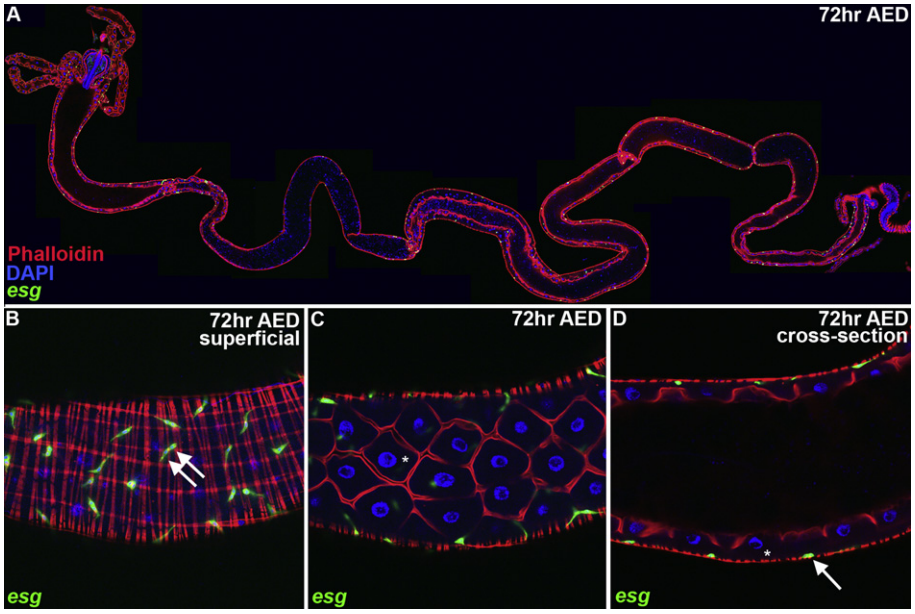

Fig. 3. *esg*$^{+}$ cells expand symmetrically in P2. (A–D) *esg*$^{+}$ cells are distributed along the length of the 72 h AED *esg > GFP* midgut (phalloidin, red; anti-GFP, green; DAPI, blue). (A) Composite micrograph; original magnification, 20×. (B–D) A series of progressively deeper optical sections from a region in the midgut (superficial to cross-section). Single *esg*$^{+}$ cells and dividing "doublets" can be detected at a basal position adjacent to the surrounding muscle. Arrows indicate *esg*$^{+}$ cells and asterisks indicate differentiated cells of the larval midgut. Original magnification, 40×.

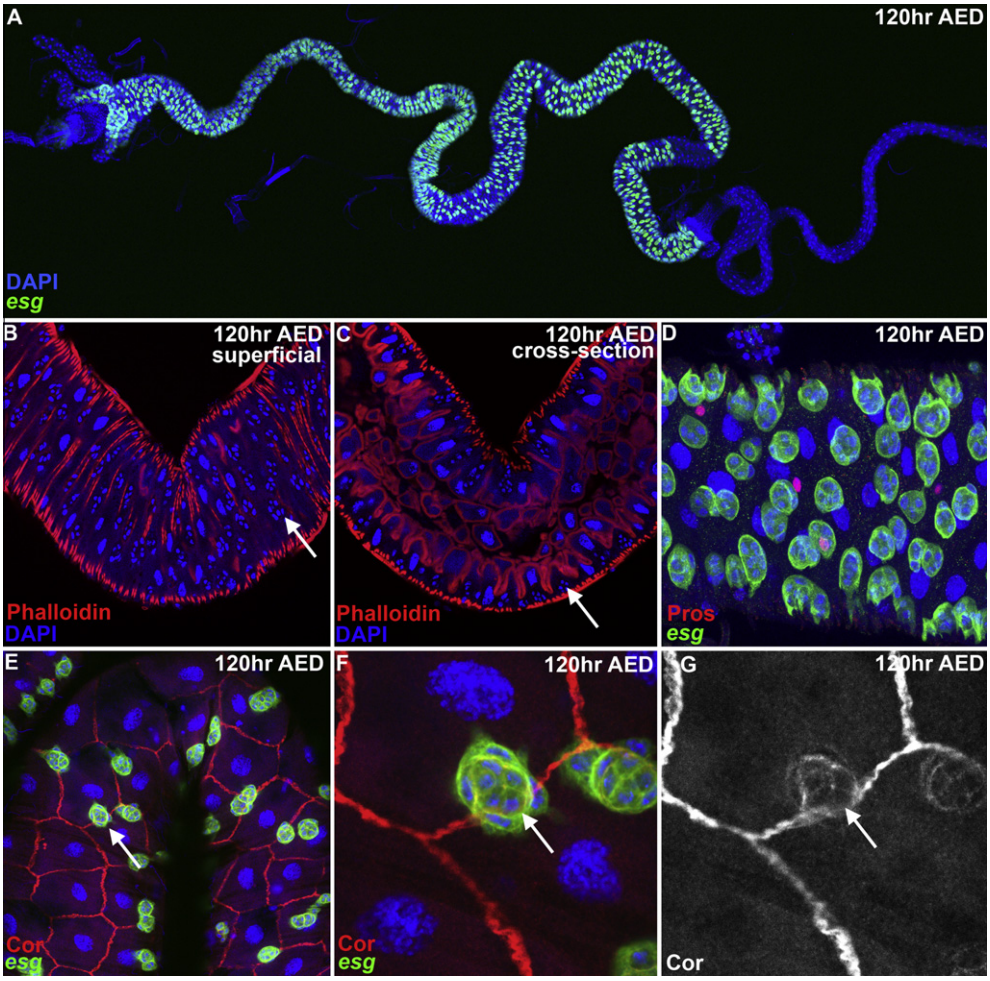

Fig. 4. *esg*$^{+}$ cells expand to form adherent clusters in P3. (A–G) 120 h AED midguts. (A) *esg* > *GFP* midgut. Composite micrograph; original magnification, 10×. (B and C) Wild type midgut contains many basally located clusters of small nuclei (phalloidin, red; DAPI, blue), arrows. Original magnification, 40×. (B) Superficial. (C) Cross-section. (D) *esg* > *GFP*. AMPs form clusters of *esg*$^{+}$ cells (anti-Pros, red; anti-GFP, green; DAPI, blue). Original magnification, 40×. (E–G) AMP clusters label positively for the septate junction marker Coracle (anti-Cor, red; anti-GFP, green; DAPI, blue). (E) Original magnification 40×. (F) Original magnification 160×. (G) Single channel.

addition, marked lineages were often present in adjacent strings of 4–11 clusters, suggesting that individual P1 AMPs exhibit different proliferative capacities prior to cluster production. These data are consistent with the observation that *esg*$^{+}$Pros^{-} cells undergo roughly four doublings on average during P1 (Fig. 1C). As lineage tracing by mitotic recombination requires cell cycle progression, these data show that P2 clusters arise from cell proliferation during P1–2; BrdU labeling experiments performed during larval stages are in agreement with this conclusion (Supplemental Fig. 3).

We next asked whether there is a direct lineage relationship between P2 clusters and the cells of the adult midgut. Experiments in which midguts were labeled at mid P2 and examined in adult midguts 2 days after eclosion showed that labeled cell lineages give rise to the cells of the adult midgut (Fig. 2B). Morphological evidence suggests that adult progenitors and differentiated cells all descend from lineages marked at P2 (Fig. 2B; arrows and asterisks). Thus, P2 clusters are comprised of cells that will form the adult midgut.

Analysis of marker gene expression in conjunction with MARCM lineage tracing experiments, suggest that the single cells detected at P1 define the midgut AMPs. To test this possibility directly, we conducted a series of directed lineage tracing experiments. A permanent genetic lineage marker *act5C* > *stop* > *lacZ*$^{nuclear(nuc)}$ (Struhl and Basler, 1993) was used to label cells in the presence of UAS-*flipase* (*flp*). First, *esgGal4* was crossed to the lineage marker to identify all cells in the adult midgut derived from the *esg*$^{+}$ population. These labeling experiments showed that almost all cells of the adult midgut were labeled (data not shown). Next, the conditionally active transgene, *esg*^{Gal4}*tubGal80*^{TS} (*esg*^{TS}), was crossed to the lineage marker to more finely map the identity of larval AMPs. In contrast to unshifted controls, a 24 h labeling pulse ending at P1 was sufficient to label most cells in the adult midgut (Fig. 2C and D). These experiments demonstrate that a population of *esg*$^{+}$ cells at embryonic/larval stages defines the AMPs.

Finally, we wished to address the lineage of Pros^{+} cells in the midgut. We considered two different possible outcomes. As previously indicated, Pros has been suggested to mark AMPs early, during embryogenesis (Oliver et al., 1993; Spana and Doe, 1995; Hirata et al., 1995). In contrast, our marker analysis in larval and pupal stages shows that Pros^{+} cells are almost completely lost from the midgut by 24 h APF (Fig. 1C). If Pros^{+} cells mark embryonic AMPs, then we predict that labeled Pros lineages should mark the entire adult midgut. If Pros^{+} cells do not label early AMPs, then we predict that only a small subset of adult midgut cells should be labeled. To distinguish between these possibilities, we sought to conduct a targeted lineage tracing experiment of the Pros^{+} population. However, control experiments comparing the *prosGal4* driver line with Pros protein distribution in the WPP midgut revealed a disparity in expression pattern (data not shown), precluding further lineage-tracing analysis.

1.3. Morphogenesis of the midgut

1.3.1. Larval

A number of steps in midgut development have been described (Robertson, 1936; Miller, 1950; Jiang et al., 1997; Jiang and Edgar, 2009). However, given the primacy of microenvironment to stem and progenitor cell behavior, we wished to re-examine the gross morphogenic changes in the midgut in relation to the dynamics and location of individual AMPs during larval and pupal periods. To establish the overall relationship between the AMPs and the gross changes in the midgut, we first plotted midgut length as a function of time. These measurements show that midgut size changes over an order of magnitude and positively correlates with AMP dynamics (Fig. 1C). These findings are also consistent with the finding that *esg*$^+$ cells define the population of AMPs.

Next, we examined the position of AMPs in the midgut from P1–3. In P1, AMPs were found to be in close proximity to the surrounding musculature and basement membrane (Fig. 1B, Supplemental Fig. 1). Overall midgut length increases fourfold and subtle changes are evident in the AMPs; single ovoid cells detectable at 24 h AED often exhibit thin processes by 48 h AED. By 72 h AMPs are often detected as dividing doublets that are distributed in alternating banding pattern along the AP axis (Fig. 3A–D; data not shown). From mid P2 to P3, midgut length decreases by roughly half from its maximum and AMPs are detected as clusters of cells (Fig. 4A).

Inspection of P3 clusters morphology indicated a degree of organization (Fig. 4B–G). Each cluster is closely associated with the basement membrane, yet the extent of contact for each cell in the cluster appeared to vary. For example, clusters often appear as rosettes consisting of both inner and outer cells (Fig. 4F); between one and three outer cells could be observed to surround the inner cells at the early P3. Outer cells appear to encapsulate inner cells; this morphology suggests a supportive or protective function. BrdU labeling also suggest that outer cells have a distinct cell cycle regulation (Supplemental Fig. 3). In addition to mere proximity, examination of a panel of junctional markers including Coracle, a septate junction marker, suggests that cells of the cluster are adherent (Fig. 4E-G). Thus, clusters consist of an adherent mass of at least two distinct cell types.

1.3.2. Pupal

During P3 midgut length declines precipitously (Fig. 1C, Fig. 5). This compaction is associated with two concomitant processes; cluster union and the delamination of cells into the luminal space. Initially, the lateral edges of *esg*$^+$ outer cells display multiple processes and begin to spread out along the basement membrane until they contact neighboring clusters. This process continues until all clusters have consolidated (Fig. 5). Upon viewing the gut in cross-section, it appears that clusters have invaded the junction between the larval midgut and the basement membrane; clusters now form a multilayer sheet situated between the musculature and the larval midgut (Fig. 5). Beginning in a localized region at first, cells delaminate into the luminal space. This process occurs within the layer of fused clusters; some of the cells remain adherent to the surrounding basement membrane and others are shed into the lumen along with the larval midgut (Fig. 5). At present, it is unclear how this cell sorting is regulated, although it is possible that the outer cells of the AMP clusters preferentially sort to the

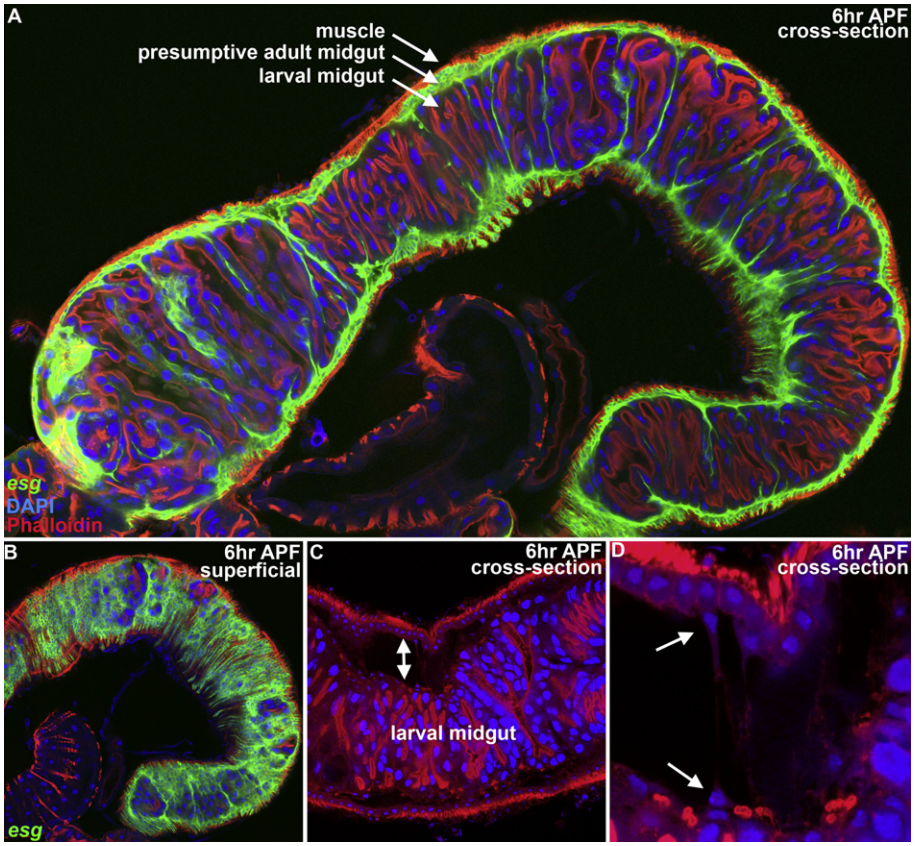

Fig. 5. Adult midgut epithelium formation following consolidation of *esg*$^+$ clusters. (A and B) *esg* > *GFP* midguts at 6 h APF. (A) Cross-section. The midgut has decreased in length and three distinct layers are evident, an outer layer of musculature, a middle layer of *esg*$^+$ cells, and an inner layer consisting of the larval midgut, arrows. *esg*$^+$ cells can often be observed to consist of two or more layers. Composite micrograph; original magnification, 20×. (B) Optical section showing middle layer of *esg*$^+$ cells. Original magnification, 20×. (C, D) Wild type midguts at 6 h APF (phalloidin, red; DAPI, blue). (C) Cross-section, original magnification 20×. The larval midgut has begun to delaminate into the midgut lumen, arrows. (D) Cross-section, original magnification 160×. Note that some small nuclei appear to delaminate along with the larval gut, arrows.

midgut lumen. By the end of P3 the larval midgut has fully delaminated into the lumen forming the yellow body (Robertson, 1936; Fig. 6). Thus, the adult midgut epithelium arises.

The early P4 midgut displays several unique features (Fig. 1C; Fig. 6). Midgut length now attains its minimum. In addition, the midgut defines a nearly autonomous epithelial envelope that is only very weakly associated with the fore- and hindgut structures. Finally, the midgut is organized as a simple columnar epithelium with basally localized nuclei and a strong band of apical actin (Fig. 6A and D). It is at this stage that individual *esg*$^{+}$Pros^{-} cells once again become detectable among the cells of the midgut epithelium, although low levels of *esg* expression can still be detected throughout the monolayer as well as in a thin sheet of cells surrounding the yellow body (Fig. 6A–D). As in the case of the larval and adult midgut, *esg*$^{+}$ cells are basally located and appear to be in contact with the visceral muscle or basement membrane, where they remain through subsequent pupal stages (Fig. 6D). During the remainder of P4 and P5 the midgut becomes progressively longer and adopts the looped configuration that is characteristic of the adult (Fig. 7; Supplemental Figs. 5 and 6). A combination of proliferation, cell shape change and growth likely account for these later changes in the midgut. We note that a distinct population of Pros^{+} cells is specified between 72–96 h APF in the pupal midgut prior to eclosion in a pattern very similar to the enteroendocrine cells of the adult midgut (Supplemental Fig. 4).

1.4. Ecdysone regulates AMP expansion

To identify signal transduction pathways required for AMP expansion we initiated a genetic screen (Supplemental Table 1). Conditional activation of transgene expression was achieved using *esg*^{TS}. Using this approach, we identified a requirement for signaling through the 20-hydroxyecdysone (ecdysone) receptor (EcR) for larval viability following expression of a dominant negative form of the receptor, when function was abrogated beginning at P1. Given that ecdysone is a steroid hormone known to coordinate the timing of multiple developmental events we sought to characterize this phenotype in greater detail.

To analyze the effects of conditional expression of dominant negative EcR transgenes on AMP expansion we first conducted a series of temperature shift experiments to systematically determine the conditions under which EcR transgenes could be activated, without affecting the developmental schedule of the larvae (see Section 3; Cherbas et al., 2003). Our studies showed that shifting larvae to the non-permissive temperature at early P2 did not significantly disrupt the duration of larval development for all transgenes analyzed. This finding is consistent with the observations that ecdysone titer exhibits a series of peaks at the onset of each larval instar required for molting (Riddiford, 1993).

EcR encodes three distinct isoforms, EcR-A, EcR-B1, EcR-B2, through the use of alternative promoters and splicing (Talbot et al., 1993). To determine the requirement of EcR in AMP expansion we tested a series of six dominant negative constructs designed to specifically block EcR activity in an isoform- specific manner (Hu et al., 2003; Cherbas et al., 2003; Brown et al., 2006). Examination of midguts at early P3 indicated that, in contrast to controls, abrogating EcR signaling led to a decrease in the AMP cluster size (Fig. 8A–G). Quantitation of the number of cells per cluster supported these observations. For each EcR transgene tested, a significant decrease in AMP number was detected

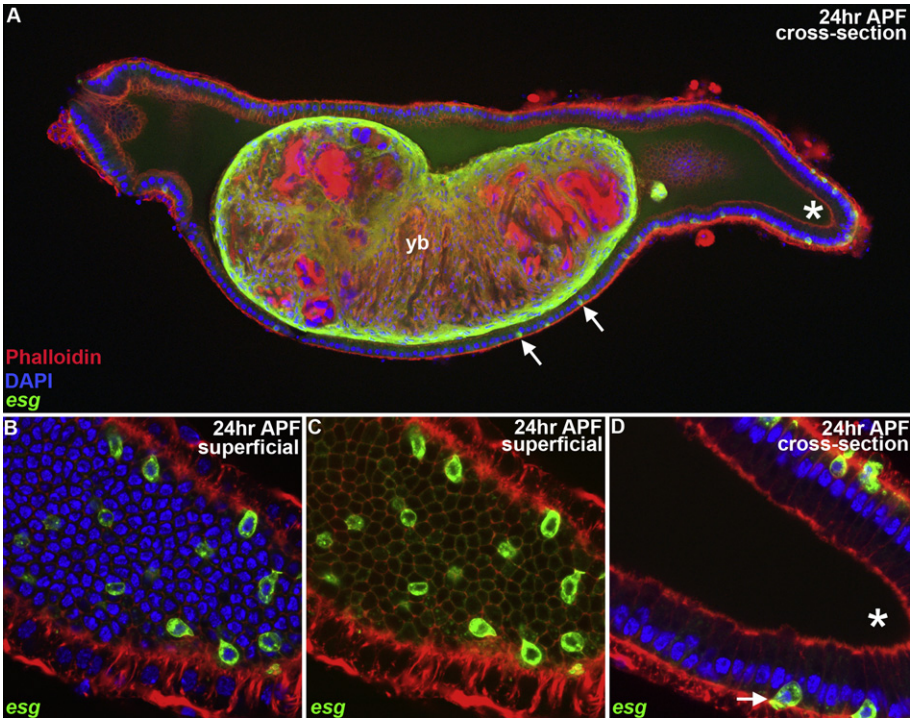

Fig. 6. Single *esg*$^{+}$ cells are present in the midgut epithelium by late P3. (A–D) *esg* > *GFP* midgut at 24 h APF (phalloidin, red; anti-GFP, green; DAPI, blue). (A) Cross-section. The midgut has decreased in length and three distinct layers are evident, an outer layer of musculature, a closely associated epithelial layer, and an inner layer consisting of the fully delaminated larval midgut called the yellow body. Single *esg*$^{+}$ cells are again detectable in the midgut epithelium at a basal position, arrows. Note, the yellow body is surrounded by *esg*$^{+}$ cells; it is possible that these cell previously surrounded AMP clusters. The foregut and hindgut are loosely associated with the midgut at this stage and do not form a continuous tube. Note anterior opening at the presumptive for/midgut boundary and closed tube at presumptive mid/hindgut boundary (asterisk). Composite micrograph; original magnification, 20×. (B–D) Original magnification, 160×. (B) Section showing single cells expressing high levels of *esg*. (C) Low levels of *esg* can be detected in all cells of the epithelium. (D) Cross-section shows that *esg*$^{+}$ cells lie in a basal position in close association with surrounding muscle. Note the ordered columnar epithelium of the midgut with high levels of apical F-actin and basally located nuclei.

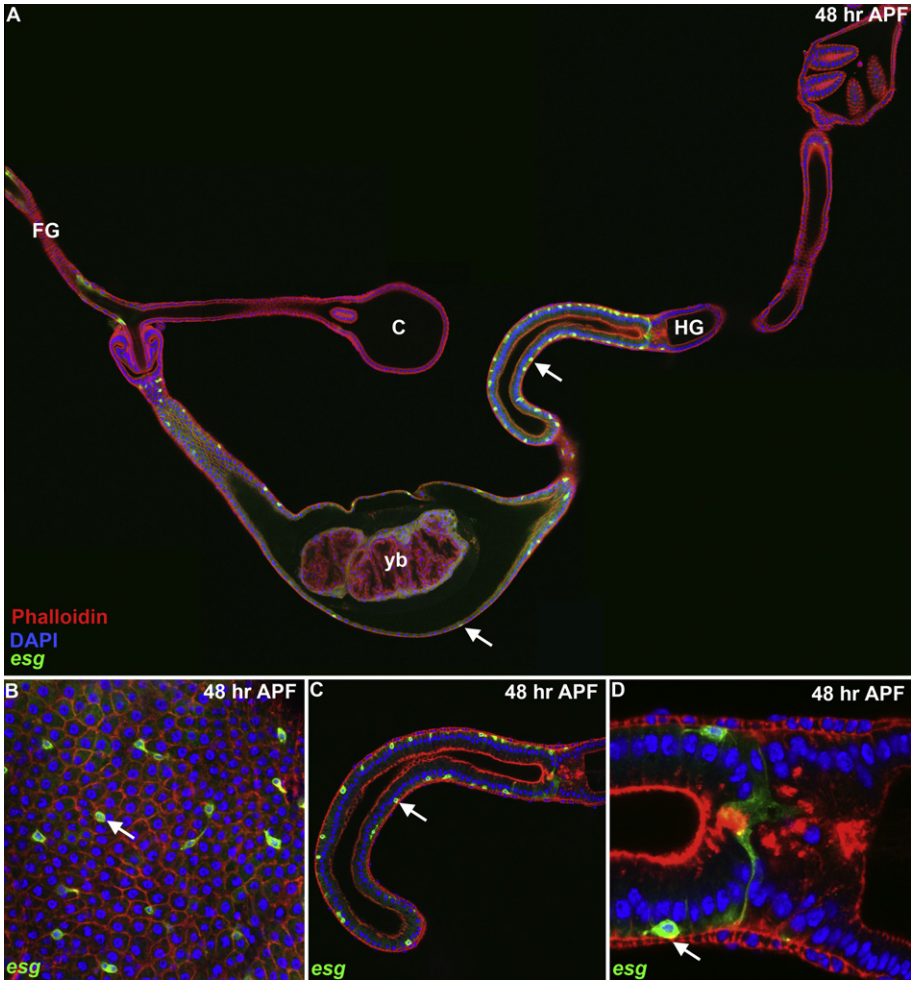

Fig. 7. *esg*$^+$ cells expand in P4. (A–D) *esg* > *GFP* midgut at 48 h APF. (A) Cross-section. Note that the yellow body is present. The foregut and hindgut are associated with the midgut. In the anterior the foregut has invaded and the crop and cardia have formed; the midgut and hindgut are not continuous. Composite micrograph; original magnification, 20X. (B) Superficial section showing single *esg*$^+$ cells, arrow. Larger DAPI positive nuclei are detectable. Original magnification, 80×. (C and D) Cross-section shows that *esg*$^+$ cells lie in a basal position in close association with surrounding muscle, arrow. (C) Original magnification, 40×. (D) Original magnification, 160×. A cellular septum separates the midgut and hindgut. Actin rich vacuoles or puncta are present in this region.

(Fig. 8H). Occasionally, cells with larger nuclei were detected among the AMP clusters. No obvious change in the number of AMP clusters was observed. These experiments suggest that EcR is specifically required for AMP expansion during the P2 expansion.*esg* is expressed in a number of distinct tissues during larval development, leaving open the possibility that the effect of EcR on AMP expansion is not direct. To directly test if ecdysone signaling is required specifically in AMPs, we conducted a mosaic analysis using the MARCM system. Examination of mosaic midguts at early P3 indicated that, in contrast to wild type controls, abrogating EcR signaling led to a decrease in the AMP cluster size (Fig. 9A–D). This effect was also evident when comparing mosaic clusters to adjacent wild type clusters within a given midgut (Fig. 9C). Quantitation of the number of cells per cluster supported these observations. Using this mosaic approach, each EcR transgene tested led to a significant decrease in AMP number (Fig. 9D and data not shown). Taken together, our analysis suggests that EcR signaling is required for AMP expansion.

2. Discussion

Here we present a series of experiments designed to more precisely define the cells that give rise to the adult midgut. We employ a two-pronged approach: defining candidate cell populations based on the expression of molecular markers, in conjunction with directed lineage tracing experiments. Using this method we define AMPs at the embryonic/larval transition. AMPs were found to have five distinct phases of activity (P1–5) between the end of embryogenesis and adulthood (see also, Jiang and Edgar, 2009; Mathur et al., 2010). Despite extensive changes in overall midgut morphology, AMPs were found to reside in the same microenvironment within the midgut. Finally, we provide evidence that an EcR-dependent signal regulates the expansion of larval AMPs.

2.1. Molecular markers of AMPs

A screen of candidate marker genes reveals that three distinct populations of small basally localized cells can be detected in the midgut at the embryonic/larval transition. Directed cell lineage-tracing analysis shows that *esg*$^+$ cells give rise to the adult midgut. Thus, *esg* is the first validated marker of larval AMPs. These lineage-tracing studies are in agreement with a recent characterization of *esg* expression in the midgut (Jiang and Edgar, 2009).

Several previous studies have noted the presence of Pros$^+$ cells in the embryonic midgut (Oliver et al., 1993; Spana and Doe, 1995; Hirata et al., 1995). In the larval midgut we observe two

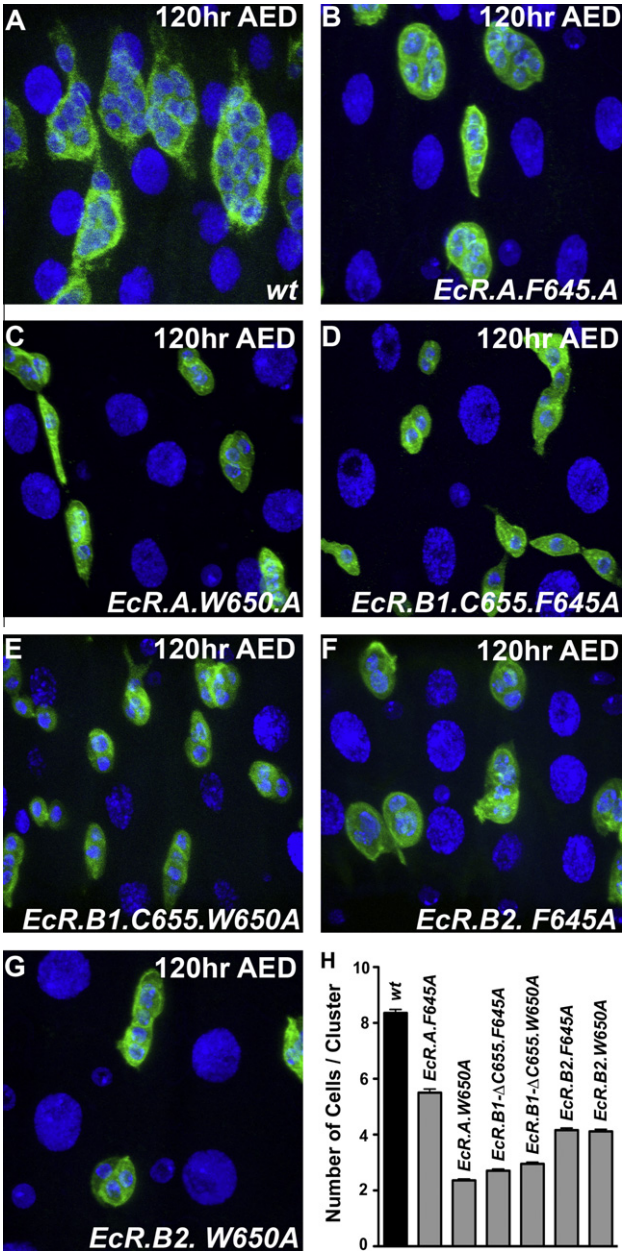

Fig. 8. EcR is required for *esg*$^{+}$ cluster expansion. (A–H) Conditional expression of dominant negative forms of EcR using *esg*^{TS} leads to a reduction in the number of cells per AMP cluster in 120 h AED midguts. Original magnification, 160×. (A) Wild type. (B) *EcR.A.F645A*. (C) *EcR.A.W650A*. (D) *EcR.B1-Δ655.F645A*. (E) *EcR.B1-Δ655.W650A*. (F) *EcR.B2.F645A*. (G) *EcR.B2.W650A*. (H) Quantitation. Compared to wild type, significant reductions in the number of cells per cluster were observed for each dominant negative EcR construct tested. Error bars denote s.e.m.

classes of Pros^{+} cells, Pros^{+} cells and *esg*$^{+}$Pros^{+} double positive cells. These observations raised the possibility that Pros expression precedes or is coexpressed with *esg* in early AMPs, however technical limitations prevented a direct experimental test of this idea. We note that by mid P1 the number of both Pros^{+} and *esg*$^{+}$Pros^{+} cells has stabilized and speculate that this later expression marks a differentiated midgut cell type(s), as these cells appear to be lost during metamorphosis (P3) along with the rest of the larval midgut (Fig. 1). Previous analysis of the adult midgut has led to the suggestion that Pros marks a population of enteroendocrine cells (Micchelli and Perrimon, 2006; Ohlstein and Spradling, 2006), raising the possibility that Pros also marks enteroendocrine cells of the larval and late pupal midgut.

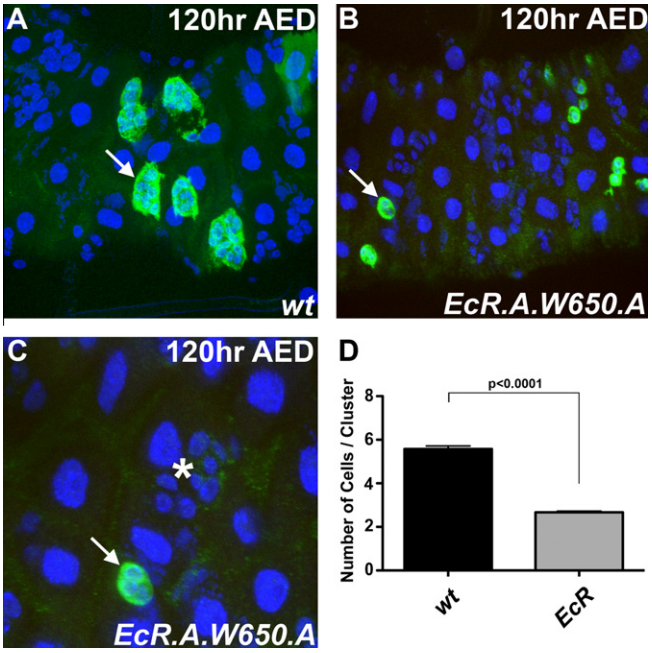

Fig. 9. EcR is required in midgut AMPs. (A–D) The MARCM system was used to positively mark AMP lineages with GFP (anti-GFP, green). (A) Wild type clones generated in P1 (24 h AED) were analyzed 120 h AED, arrow. Original magnification, 80×. (B) Dominant negative *EcR.A.W650A* clones generated at P1 and analyzed 120 h AED result in reduced AMP cluster size, arrow. Original magnification, 80×. Similar results were observed with all other EcR constructs (data not shown). (C) High magnification of *EcR.A.W650A* clone shown in panel B. Note the greater number of cells present in an adjacent wild type cluster (asterisk). Original magnification, 160×. (D) Quantitation. Compared to wild type, a significant reduction in the number of cells per cluster was observed in *EcR.A.W650A* clones. Error bars denote s.e.m.

2.2. Phases of AMP activity

Time resolved analysis of marker gene expression during larval and pupal stages indicates five phases of AMP activity. These phases suggested themselves on the basis of relative changes in the number of cell populations expressing different marker profiles and overall morphogenesis of the midgut. Thus, these are not absolute distinctions, but reflect general trends in AMP activity. For example, beginning in the middle of P1, AMPs appear to undergo a series of apparently symmetric divisions rapidly expanding their numbers within the tissue. However, by mid P2 this pattern of division has changed to include the production of daughters within AMP clusters. Following metamorphosis in P3 where differentiated cells of the larval gut are shed, a similar process is repeated. Symmetric expansion of AMP pool during early P4 is followed by the production of distinct Pros^{+} daughter cells by mid P5. We note that the number of AMPs produced by the end of P1 is roughly equivalent to the number produced by the end of P5, suggesting tight regulation. Thus, AMPs demonstrate the ability to reversibly switch between expansionary divisions and divisions yielding differentiated daughters in both larval and pupal stages. It remains unclear if there is a common molecular mechanism underlying this behavior.

2.3. AMPs: stem or progenitor cells

Stem cells undergo self-renewal and give rise to differentiating cells types. As such, stem cell establishment can be defined as the point at which these processes commence. Thus, it is possible that ISCs are already established in the midgut by P1; alternatively ISCs are established at a later time point, as previously suggested (Jiang and Edgar; 2009). Current data does not unambiguously

discriminate between these possibilities. However, our investigation has led us to favor the former model for several reasons. First, in the cases where stem cells have been precisely characterized, microenvironment is known to be of primary importance in maintaining stem cell fate (Morrison and Spradling, 2008). We show that by P1, AMPs are localized to a distinct basal position in the midgut adjacent to the surrounding musculature and basement membrane where they remain through the succession of developmental events and the place adult ISCs are known to reside (Micchelli and Perrimon, 2006; Ohlstein and Spradling, 2006). Second, AMPs undergo a rapid expansion during P1 and P2. In addition, activation of EGF signaling causes AMP hyperplasia (Jiang and Edgar, 2009), indicating that AMPs harbor an even greater capacity for expansion than normally expressed. Third, AMPs generate daughter cells with distinct morphologies within P3 clusters suggesting that AMPs produce differentiated daughters. Fourth, tests of candidate genes show that AMPs express *esg* as early as P1, the first characterized marker of adult ISCs (Micchelli and Perrimon, 2006). Thus, we favor the view that ISCs are established the first time they adopt their basal position in the midgut and their stage specific lineal output is regulated by the changes in tissue architecture imposed by morphogenesis of the larval and pupal midgut. If true, establishment of ISCs in the midgut would parallel recent studies of male germline demonstrating GSC establishment during embryogenesis (Sheng et al., 2009). Finally, it is possible that ISCs are specified early, but other cells within the AMP cluster retain the capacity to acquire ISC characteristics, thereby buffering the system against developmental stress. Distinguishing these possibilities will require more highly resolving assays to measure self-renewal at different developmental stages.

2.4. Ecdysone signaling regulates AMP expansion

A large body of evidence shows that ecdysone acts broadly on different larval tissues to coordinate the events of morphogenesis. Here we demonstrate that reduction of ecdysone signaling by overexpressing dominant forms of EcR under the control of esg^{TS} decreases the number of AMPs. Our findings are consistent with a number of previous studies in the midgut (Jiang et al., 1997; Hall and Thummel, 1998; Li and Bender, 2000; Li and White, 2003). These studies have relied on global reductions in ecdysone signaling using either specific EcR alleles or isoform specific rescue to circumvent early lethality. Expression analysis shows that EcR isoforms exhibit differential expression in the midgut (Talbot et al., 1993). Together these studies support a model in which ecdysone acts directly on AMPs to regulate expansion and midgut morphogenesis (Jiang et al., 1997; Li and White, 2003). Here a direct test suggests that this is, in fact, the case, as mosaic reductions in EcR activity in the midgut affected AMP cluster expansion.

3. Methods

3.1. Fly Strains

The following fly strains were used: y, w, UAS-GFP, hsflp; tubGal4, FRT^{82B}, tubGal80/TM6B. w; FRT^{82B} hsπM and w^{1118} as wild type controls. w; esg-Gal4/ CyO. y, w; esg^{K606}/CyO (esg-lacZ). act5C > stop > $lacZ^{nuc}$ (lineage tracer). UAS-GFP. UAS-flp. $tubGal80^{TS}$. $pros^{Gal4}$. UAS-EcR.A.F645A. UAS-EcR.A.W650A. UAS- EcR.B1-Δ655.F645A. UAS-EcR.B1-Δ655.W650A. UAS-EcR.B2.F645A. UAS-EcR.B2.W650A. See FlyBase for further information at http://flybase.org.

3.2. Staging

Larvae of specified stage were obtained in the following manner. A ~20 h egg lay was collected and embryos were evenly arrayed in 96 well plates containing PBS. Wells were scanned every 15–30 min to identify newly hatched first instar larvae. Second instar larvae were obtained by aging first instars for 24 h in a small, moist petri dish on a small piece of fly food at 25 °C. Third instar larvae were obtained by isolating late second instar larvae, placing them on a piece of fly food in a petri dish and then returning to inspect larvae every 15–30 min to identify individuals that have progressed to third instar on the basis of spiracle morphology. Pupae of the desired stage were obtained by isolating white prepupae (WPP) from low-density cultures and aging them at 25 °C on the wall of a fresh vial for the desired period.

3.3. Lineage analysis

3.3.1. MARCM

Flies were allowed to lay eggs for four days in the same vial. Vials were cleared and heat shocked for 1 h at 37 °C to induce mitotic recombination. WPP were collected 3 days after heat shock to recover individuals induced at the beginning of second instar or 4 days after heat shock to recover individuals induced at the beginning of first instar. Lineage tracing experiments presented in Fig. 2B were performed by selecting induced WPP and aging them for 1–2 days following eclosion at 25 °C prior to dissection.

3.3.2. Directed lineage tracing

The lineage tracing strain *act > stop > $LacZ^{nuc}$*; *UAS-flp* was crossed to the appropriate Gal4 driver. esg^{+} lineages were traced by crossing the lineage tracer to either esg^{Gal4} or esg^{TS}. In the latter case, 24 h egg collections were collected at 29 °C and subsequently cultured to eclosion at 18 °C. $Pros^{+}$ lineages were traced by crossing the lineage tracer to $pros^{Gal4}$; midguts were analyzed from both 48 h APF pupae and adults 1–2 days after eclosion.

3.4. Temperature shift analysis

Initial screen of pathway components was performed by collecting 48 h egg lays from the appropriate crosses at 18 °C and shifting the vials to 29 °C. To analyze the effect of expressing dominant negative EcR transgenes using the conditional esg^{TS} allele, appropriate crosses were established and allowed to lay eggs for one day at 18 °C. Vials were cleared after one day and kept at 18 °C for five additional days. On the 6th day at 18 °C, vials containing early third instar larvae were shifted to 29 °C. WPP were collected after 2–3 days at 29 °C to ensure that the individuals analyzed had not been developmentally delayed.

3.5. Histology

3.5.1. Sample preparation

Adult flies were dissected in 1× PBS (Sigma, USA). The gastrointestinal tract was removed and fixed in a final solution of 0.5× PBS (Sigma, USA) and 4% electron microscopy grade formaldehyde (Polysciences, USA) for a minimum of 30 min. Samples were washed in 1× PBS + 0.1% Triton X100 (PBST) for 2 h, then incubated with primary antibodies overnight. Samples were washed in PBST for 2 h then incubated with secondary antibodies for 3 h. Finally, samples were washed in PBST overnight. Mounting media containing DAPI (Vectashield, USA) was added and samples were allowed to clear for 1 h prior to mounting. All steps were completed at 4 °C with no mechanical agitation.

3.5.2. Antisera

3.5.2.1. Primary antibodies. Chicken anti-GFP (Abcam, USA) used at a dilution of 1:10,000; rabbit anti-β-Gal (Cappel, USA), 1:2000; mouse anti-β-Gal (Developmental Studies Hybridoma Bank; DSHB), 1:100; mouse anti-Pros (DSHB) 1:100; rabbit anti-Asense,

1:5000 (generous gift of Y. Jan); anti-Coracle 1:500 (generous gift of R. Fehon).

3.5.2.2. Secondary antibodies. Goat anti-chicken Alexa 488 (Molecular Probes, USA) used at a dilution of 1:2000; goat anti-mouse Alexa 568 (Molecular Probes, USA), 1:2000; goat anti-mouse Alexa 633 (Molecular Probes, USA), 1:2000; goat anti-rabbit Alexa 568 (Molecular Probes, USA), 1:2000.

3.5.3. Mounting media and dyes

Vectashield + DAPI mounting media (Vector, USA). Alexa 568 Phalloidin (Molecular Probes, USA), 1:2000.

3.5.4. Microscopy and Imaging

Samples were examined on a Leica DM5000 upright fluorescent microscope. Confocal images were collected using a Leica TCS SP5 confocal microscope system. Images were processed for brightness and contrast and assembled in Photoshop CS (Adobe, USA).

3.5.5. Cell counts, measurements and analysis

The cell numbers in Fig. 1 were obtained by counting both sides of the 1st and 2nd instar midguts, which their small size easily permitted. Only the side of the gut in contact with the cover slip was counted for all remaining stages. This value was then doubled to provide an estimate of the total cell number in the midgut for each marker. Counting started at the base of the gastric caeca (or cardia) and ended at the pylorus. Both male and female larvae were counted and pooled. Midgut length was determined using by analyzing 5× images of each midgut using LAS-AF software (Leica, Germany).

The counts in Figs. 8 and 9 were obtained from midguts in which only cells on the surface of each sample closest to the cover slip were analyzed. The number of cells was determined by counting $DAPI^+$ nuclei. AMP clusters that had begun to join with their neighbors were excluded from the analysis. In Fig. 8, a single 40× frame immediately anterior to the pylorus was scored on a compound fluorescence microscope for each sample analyzed. In the mosaic analyses, clones were scored irrespective of their anterior-posterior position along the midgut.

The counts shown in Supplemental Fig. 2 were obtained by taking confocal images from three defined regions along the length of the WPP midgut for each sample analyzed; anterior, middle and posterior. The number of $DAPI^+$ nuclei was counted directly from these micrographs. As such these values represent a low estimate of actual AMP numbers. All *t*-tests were performed using Prism (GraphPad Software, USA).

Note in press

As we were preparing this manuscript, two related studies on AMPs have been published (Jiang and Edgar, 2009; Mathur et al., 2010).

Acknowledgments

We thank G.-H. Baeg, S. Benzer, C. Doe, T. Lee, and the Bloomington stock center for generously providing *Drosophila* strains; R. Fehon, Y. Jan, and Developmental Studies Hybridoma Bank for generously providing antibodies. We thank members of the Micchelli lab for comments and discussion. N.P. is an HHMI investigator. C.A.M. is a Pew Biomedical Research Scholar. Additional research funding for this work was provided by the Harvard Stem Cell Institute (C.A.M.), the Stem Cell Research Foundation (C.A.M.) and the American Cancer Society (C.A.M.).

Appendix A. Supplementary data

Supplementary data associated with this article can be found, in the online version, at doi:10.1016/j.gep.2010.08.005.

References

Brand, M., Jarman, A.P., Jan, L.Y., Jan, Y.N., 1993. Asense is a Drosophila neural precursor gene and is capable of initiating sense organ formation. Development 119, 1–17.
Brown, H.L., Cherbas, L., Cherbas, P., Truman, J.W., 2006. Use of time-lapse imaging and dominant negative receptors to dissect the steroid receptor control of neuronal remodeling in Drosophila. Development 133, 275–285.
Cherbas, L., Hu, X., Zhimulev, I., Belyaeva, E., Cherbas, P., 2003. EcR isoforms in Drosophila: testing tissue-specific requirements by targeted blockade and rescue. Development 130, 271–284.
Hall, B.L., Thummel, C.S., 1998. The RXR homolog ultraspiracle is an essential component of the Drosophila ecdysone receptor. Development 125, 4709–4717.
Hartenstein, A.Y., Rugendorff, A., Tepass, U., Hartenstein, V., 1992. The function of the neurogenic genes during epithelial development in the Drosophila embryo. Development 116, 1203–1220.
Hirata, J., Nakagoshi, H., Nabeshima, Y., Matsuzaki, F., 1995. Asymmetric segregation of the homeodomain protein prospero during Drosophila development. Nature 377, 627–630.
Hu, X., Cherbas, L., Cherbas, P., 2003. Transcription activation by the ecdysone receptor (EcR/USP): identification of activation functions. Mol. Endocrinol. 17, 716–731.
Jiang, H., Edgar, B.A., 2009. EGFR signaling regulates the proliferation of Drosophila adult midgut progenitors. Development 136, 483–493.
Jiang, C., Baehrecke, E.H., Thummel, C.S., 1997. Steroid regulated programmed cell death during Drosophila metamorphosis. Development 124, 4673–4683.
Kowalevsky, A., 1887. Beitrage zur Kentniss der nachembryonalen Entwicklung der Musciden. Zeit. wiss. Zool. 45, 542–594.
Lee, T., Luo, L., 1999. Mosaic analysis with a repressible cell marker for studies of gene function in neuronal morphogenesis. Neuron 22, 451–461.
Li, T., Bender, M., 2000. A conditional rescue system reveals essential functions for the ecdysone receptor (EcR) gene during molting and metamorphosis in Drosophila. Development 127, 2897–2905.
Li, T.R., White, K.P., 2003. Tissue-specific gene expression and ecdysone-regulated genomic networks in Drosophila. Dev. Cell 5, 59–72.
Mathur, D., Bost, A., Driver, I., Ohlstein, B., 2010. A transient niche regulates the specification of Drosophila intestinal stem cells. Science 327, 210–213.
Micchelli, C.A., Perrimon, N., 2006. Evidence that stem cells reside in the adult Drosophila midgut epithelium. Nature 439, 475–479.
Miller, A., 1950. In: Demerec, M. (Ed.), The Biology of Drosophila. Hafner, New York, pp. 420–442.
Morrison, S.J., Spradling, A.C., 2008. Stem cells and niches: Mechanisms that promote stem cell maintenance throughout life. Cell 132, 598–611.
Ohlstein, B., Spradling, A., 2006. The adult Drosophila posterior midgut is maintained by pluripotent stem cells. Nature 439, 470–474.
Oliver, G., Sosa-Pineda, B., Geisendorf, S., Spana, E.P., Doe, C.Q., Gruss, P., 1993. Prox 1, a prospero-related homeobox gene expressed during mouse development. Mech. Dev. 44, 3–16.
Perez, C., 1910. Recherches histologiques sur la metamorphose des muscides (*Calliphora erythrocephala*). Arch. Zool. Exp. Gen. 4, 274.
Riddiford, L.M., 1993. Hormones and drosophila development. In: Bate, M., Martinez-Arias, A. (Eds.), The Development of Drosophila. Cold Spring Harbor Laboratory Press, Cold Spring Harbor, New York.
Robertson, C.W., 1936. The metamorphosis of *Drosophila melanogaster*, including an accurately timed account of the principal morphological changes. J. Morphol. 59, 351–399.
Sheng, X.R., Posenau, T., Gumulak-Smith, J.J., Matunis, E., Van Doren, M., Wawersik, M., 2009. Jak-STAT regulation of male germline stem cell establishment during Drosophila embryogenesis. Dev. Biol. 334, 335–344.
Skaer, H., 1993. The alimentary canal. In: Bate, M., Martinez-Arias, A. (Eds.), The Development of *Drosophila melanogaster*, pp. 941–1012.
Spana, E., Doe, C.Q., 1995. The prospero transcription factor is asymmetrically localized to the cell cortex during neuroblast mitosis in Drosophila. Development 121, 3187–3195.
Struhl, G., Basler, K., 1993. Organizing activity of wingless protein in Drosophila. Cell 72, 527–540.
Talbot, W.S., Swyryd, E.A., Hogness, D.S., 1993. Drosophila tissues with different metamorphic responses to ecdysone express different ecdysone receptor isoforms. Cell 73, 1323–1337.
Technau, G., Campos-Ortega, J.A., 1986. Lineage analysis of transplanted individual cells in embryos of *Drosophila melanogaster*. III. Commitment and proliferative capabilities of pole cells and midgut progenitors. Wilhelm Roux' Arch. Dev. Biol. 195, 489–498.
Tepass, U., Hartenstein, V., 1994. Epithelium formation in the Drosophila midgut depends on the interaction of endoderm and mesoderm. Development 120, 579–590.
Tepass, U., Hartenstein, V., 1995. Neurogenic and proneural genes control cell fate specification in the Drosophila endoderm. Development 121, 393–405.